

The Initial Position and Postural Attitude of Vehicle Operators

H-Point and D-Point in the Pelvis

Raymond R. Brodeur, Yuntao Cui, Herbert M. Reynolds

August 15, 1995

I. Introduction

Seated posture can be accurately described when the position of the pelvis is accurately measured. The pelvis is one of the most difficult body segments to measure due to the amount of tissue overlaying it and the fact that it is a very private area of the body. To the automobile seat manufacturer, three points on the pelvis are of great importance: H-point (hip joint location) D-point (ischial tuberosity) and ASIS (anterior superior iliac spine). H-point is most important for vehicle packaging, D-point is important for comfort and safety of the occupant and the lap belt is most effective for holding the pelvis in the seat during a crash if it is below the ASIS. This report describes methods developed at the Ergonomics Research Laboratory for measuring pelvic position, using non-invasive methods for locating H-point and D-point. Results from 102 subjects are summarized, describing five points measured on each subject's pelvis and one additional point (H-point) calculated from the measured data.

The first part of this report describes the analytical methods for locating H-point from easily identified anatomical landmarks on a subject's pelvis. The analysis is based on data from Reynolds, *et al* [1], a data base that contains the three-dimensional coordinates of 118 points from 80 male and 85 female pelvises. A rigorous investigation reveals that H-point can be accurately located based on three pelvic landmarks: ASIS, and the left and right ischial tuberosities.

The second section describes the equipment and procedures for measuring anatomical landmarks on the pelvis of 102 subjects. Pressure mats (Tekscan, inc.) were used to locate the ischial tuberosities of a subject while seated on a hard seat surface. A CMM was used to measure all other pelvic landmarks: ASIS, PSIS, S1 and the greater trochanter.

In the final section, the results of the measurements are summarized, including an investigation into measurement error. The *in vivo* pelvic measurements in this study were compared to the *in vitro* measurements from the pelvic data base [1] to determine the extent of any differences between the two data sets. In addition, we describe a method for calculating a tissue correction vector to adjust for tissue and clothing over the ASIS when that landmark is measured using a 3D video-stereoscopic method (video anthropometry).

II. Materials and Methods

A. Analytical Methods: Locating H-Point from Anatomical Landmarks

In this paper, we describe an approach for locating the hip joint (H-point) of the human pelvis. We assume that the 3D location of the anterior superior iliac spine (ASIS) points and ischial tuberosity points are known. Figure 1 shows the left ASIS point (**A**), the right ASIS point (**B**), and the left ischial tuberosity (point **I**). Our goal is to determine the 3D coordinate of the hip joint point (**H** in Figure 1) based on the location of the ASIS points and ischial tuberosity points.

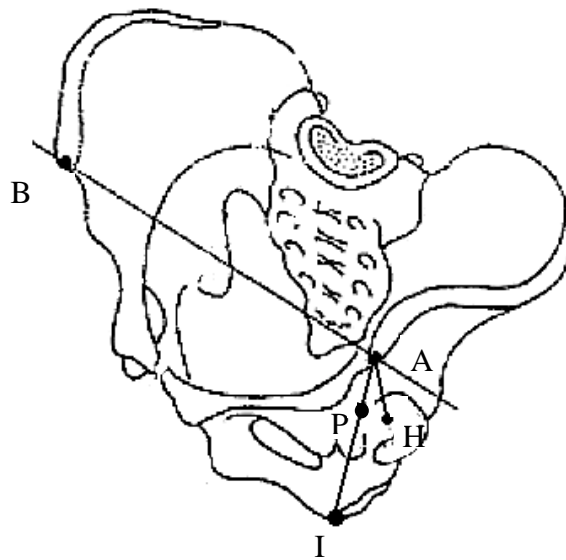


Figure 1. The human pelvis and the landmarks used to estimate H-point.

There are two parts to this analytical section. In the first part, a linear regression analysis is used to study the relation between $\|A-I\|$ and $\|A-P\|$ where $\| \ \|$ is the Euclidean distance and **P** is the projection of the hip joint (**H**) to the line **AI**. The regression study shows there is a strong relationship between $\|A-I\|$ and $\|A-P\|$. The results of the regression study provide a method for calculating the 3D coordinates of the point **P** based on the ASIS and ITCH points. In the second part of the paper, we present our approach for deriving the hip joint point **H** from the point **P**.

1. Regression Study

The male and female pelvises have quite different characteristics [2, 3]. The male acetabulum is larger than the female due to the large femoral head of the male. The inner dimensions of the pelvis are relatively and absolutely greater in the female. In the

following regression study, we divide the pelves of the Reynolds, *et al* data base [1] into two groups based on gender and, for each group, a linear regression equation is derived.

The goal of this regression study is to derive a linear relationship between $\|\mathbf{A-I}\|$ and $\|\mathbf{A-P}\|$. Using the common notation for regression analysis [4], we let $x = \|\mathbf{A-I}\|$ and $y = \|\mathbf{A-P}\|$. The linear relation which we try to establish has the form

$$y = \beta x + \alpha \tag{1}$$

A is the anterior superior iliac spine point, **I** is the ischial tuberosity point and **P** is the projection of the hip joint point to the line **AI**. For the definitions of the anterior superior iliac spine point, the ischial tuberosity point and the hip joint point, readers may refer to [2, 3].

Fitting the regression lines

The pelvis database [1] has 80 male and 85 female pelves, of which we used 73 male and 79 female pelves. Several pelves were eliminated due to missing or erroneous data. The scatter diagram and linear fit results are shown in Figure 2. For male pelves the regression equation is

$$y = 0.67x - 21.25 \tag{2}$$

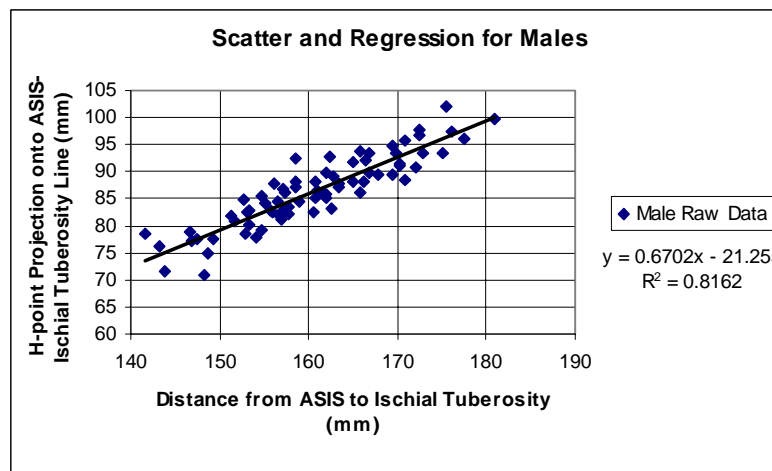
(males)

The regression equation for female pelves is

$$y = 0.68x - 17.50 \tag{3}$$

(females)

An analysis of variance (ANOVA) was performed for each of the regression lines (Table 1). The results of the F tests are included in the tables. A summary measure of goodness-of-fit that is frequently referred to in the literature is r^2 . r^2 can be thought of intuitively as the proportion of the variance of y that can be explained by the variable x . If $r^2 = 1$, then all the variation in y can be explained by the variation in x and all the data points fall on the regression line. If $r^2 = 0$, then x gives us no information about y and the variance of y is the same with or without knowing x . The r^2 value for the male and female pelves are 0.82 and 0.85, respectively.



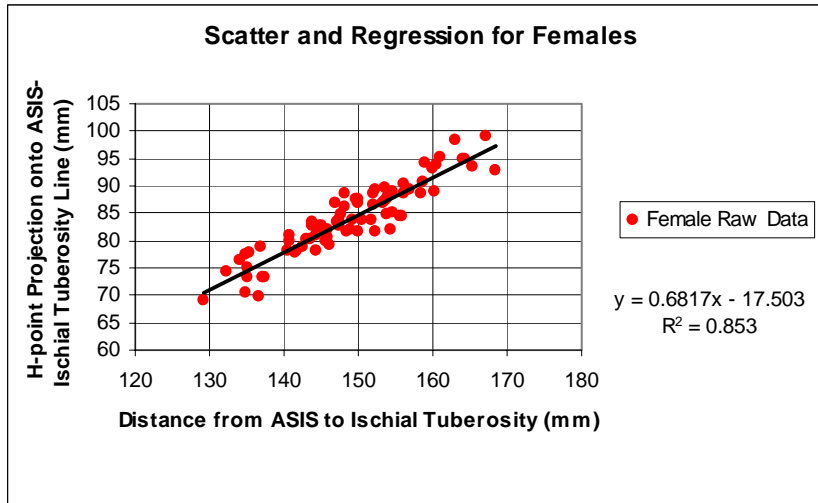


Figure 2. Scatter plots and regression lines of the projection length $\|A-P\|$ against the length of the vector $\|A-I\|$ (Male = top graph, Female = lower graph).

Male	SS	df	MS	F statistic	p-value
Regression	2508.24	1	2508.24	315.21	0.000
Residual	564.98	71	7.96		
Total	3073.22	72			
Female	SS	df	MS	F statistic	p-value
Regression	2810.62	1	2810.62	446.97	0.000
Residual	484.20	77	6.29		
Total	3294.82	78			

Table 1. ANOVA table for male (top) and female (bottom) pelves.

2. Computing the Hip Joint Point

The regression study of the previous section relates the point **P** to the anterior superior iliac spine point (**A**) and the ischial tuberosity point (**I**). The 3D coordinates of **P** can be computed using equations (2) or (3), depending on gender. In this section, we derive the 3D coordinates of the hip joint point (**H**) from point **P**.

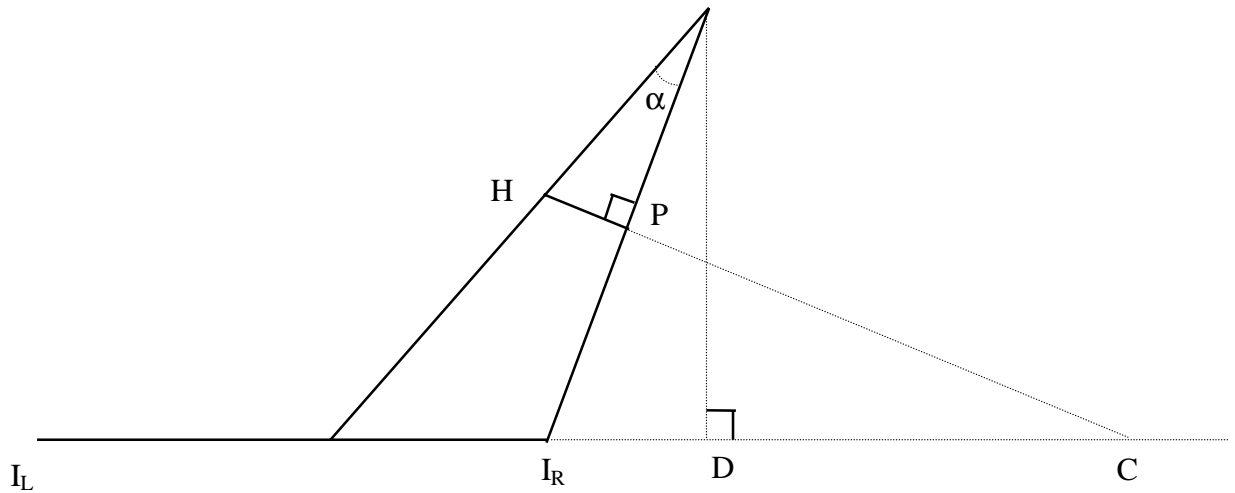


Figure 3. Illustration of the relevant points for computing hip joint point (H).

Given the 3D coordinates of the left and right ischial tuberosity points (I_L and I_R), and the right anterior superior iliac spine point (A_R), as shown in Figure 3, assume that the hip joint point H is coplanar with the points I_L , I_R and A_R and the angle α (angle between $A_R I_R$ and $A_R H$) is known. The angle α can be determined from the pelvic data base and the mean and standard deviations for males and females are summarized in Table 2. The procedure for computing the hip joint point is as follows:

1. Compute the 3D coordinates of the point P using equations (2) or (3), depending on the gender of the subject.
2. Let C be the intersection point of line segments $I_L I_R$ and HP and D be the projection of the point A on the line $I_L I_R$. The vector length $\|I_R C\|$ can be obtained as follows:

$$\|I_R C\| = (\|I_R P\| \cdot \|A I_R\|) / \|D I_R\|.$$

Then the 3D coordinate of the point C is determined by

$$C = I_L + (1 + \|I_R C\| / \|I_L I_R\|)(I_R - I_L).$$

3. Finally, the 3D coordinate of the hip joint point H is computed. According to the definition of the point P , we have HP perpendicular to AP . Therefore,

$$\|AH\| = \|AP\| / \cos \alpha$$

Then the 3D coordinate of H can be computed from

$$\mathbf{H} = \mathbf{C} + (1 + \frac{\|\mathbf{HP}\|}{\|\mathbf{PC}\|})(\mathbf{P} - \mathbf{C})$$

The above equations assume that the hip joint point \mathbf{H} is coplanar with the points \mathbf{I}_L , \mathbf{I}_R and \mathbf{A}_R . This assumption is based on an analysis of the pelvis database. If the point \mathbf{P} lies on the plane determined by the points \mathbf{I}_L , \mathbf{I}_R and \mathbf{A}_R , and the angle between the line \mathbf{AH} and the plane is θ , then the angle θ can be determined from the pelvic data base [1]. Table 2 shows the mean and the standard deviation of θ and α . Since the angle θ is small, the assumption that H-point lies on the plane defined by \mathbf{I}_L , \mathbf{I}_R and \mathbf{A}_R can be assumed to be valid.

Sex	Mean θ	Std Dev θ	Mean α	Std Dev α
Male	2.37°	2.69°	4.27°	2.08°
Female	3.91°	2.64°	6.07°	2.67°

Table 2. Mean and standard deviation of θ and α .

B. Equipment and Procedures

Measuring anatomical landmarks on the pelvis is a difficult task. In order to determine pelvic position in 3D space, at least three points on the pelvis must be measured. The most easily identifiable and accessible point is the anterior superior iliac spine (ASIS). This point has been shown to be identifiable using a video based system for measuring landmarks of the seated vehicle operator [5]. The PSIS (posterior superior iliac spine) is another possible landmark; however, in a subject sitting in a seat with a backrest, it is impossible to locate using non-invasive techniques. The ischial tuberosities can be measured in the seated posture using a pressure mat system. The ischial tuberosities are pelvic structures through which body weight is transmitted in the seat posture, and therefore, these structures define peak pressures in the seat cushion. The complete experimental protocol is described in ERL-TR-95-001. In this report we describe this technique for measuring the ischial tuberosities on the seated subject.

1. Equipment

Pressure Mat System. Placing a pressure mat [8] between a subject and a seat surface provides a means of locating and measuring the high-pressure areas under the ischial tuberosities. Tekscan pressure mats were used to locate the contact area and measure the centroid of the high-pressure peaks under the ischial tuberosities of a seated subject. Two 112mm X 112mm mats (with 1.2mm X 1.2mm sensors on 2.5mm centers, 10psi max pressure) were used (Figure 4).

CCM. The CCM (FARO Technologies) is a six-degree of freedom electrogoniometer [8] capable of measuring the three-dimensional position of a point with an error less than 0.1mm. It was used to measure the location of the anatomical landmarks illustrated in Figure 4.

Video Anthropometry. The video anthropometry system [5,6,8] is composed of four video cameras mounted in the vehicle laboratory or seat buck in standardized locations. The video cameras provide a means of measuring the three-dimensional position of any point that lies in the field of view of at least two cameras. Using this method, targets on a subject can be measured in a safe and noninvasive manner during actual highway driving.

Four CCD cameras are located as follows:

Camera	Location
1	Dome light fixture
2	A pillar above dashboard
3	A pillar below dashboard
4	B pillar, middle of window opening

Attached to the lens of each camera is an array of infrared (IR) LED's. Images from the four cameras are multiplexed by a frame grabber board in an IBM compatible 486 computer. All camera images are collected in 0.13 seconds. A generalized stereo algorithm was utilized to develop the software for image analysis. When two or more cameras observe the same target the three-dimensional coordinates can be calculated using direct linear transformation [5].

Spine Anthropometry Seat (SAS). The spine anthropometry seat [8] was used to take anthropometric measurements and for developing a model of the spinal column that predicts lumbar contour for different seated postures. In this report we concentrate on the methods, techniques and reliability of the data collected on the pelvis.

Coordinate System. Since the CMM was moved between two measurement stations (i.e. seat buck and SAS) for each subject's laboratory session, the coordinate system had to be quickly and accurately redefined. For the SAS, the origin was 14.5 cm behind the seat back and lying approximately in the mid-sagittal plane as shown in Figure 4. The +Z axis was directed upward, perpendicular to the horizontal seat surface of the SAS. +X was defined in a forward direction and +Y was defined in the left lateral direction. Thus, a right-handed, orthogonal axis system was defined that corresponded to the axes of the cardinal anatomical planes of the body (i.e. sagittal, frontal, and transverse). For the seat buck the coordinate system origin was located at the right rear seat-track bolt, with +X parallel to the right seat-track, +Y pointing toward the left seat-track and +Z running perpendicular to the plane defined by the left and right seat-tracks.

Pelvic Stabilization. A seat belt was combined with the pelvic plate shown in Figure 4 to hold the subject's pelvis in a single fixed posture. In the data analysis section we investigate the extent to which we were able to hold the pelvis in one position.

2. Pelvic Measurement Procedures

Subjects One hundred and two subjects were recruited [7,8] with ages ranging from 25 to 76. There were an equal number of males and females. After a subject arrived, the purpose and procedures of the experiment were explained and the subject signed an informed consent form approved by the MSU UCRIHS committee.

Clothing All subjects were provided biking shorts and a tank top. Shoes were removed for the pelvic and spine data collection phase of the study.

Equipment Setup The CMM was moved to a preset position and the coordinate system was defined as described above. The pressure mats were positioned as illustrated in Figure 4 and the pressure mat handles were attached. The seat height was lowered to its lowest setting and the pelvic plate was positioned to the upright position.

Subject Position The subject was asked to sit so that there were two clearly defined peak pressures on the pressure mats (Figure 4). The output of the pressure mats was shown in real time on a computer monitor and the subject position was adjusted until the high pressure areas created by the ischial tuberosities were visible. For some subjects the pressure readings were saturated beyond the range of the pressure mat, so a foam pad was placed over the pressure mats to reduce any potential for damage to the mats.

Once the subject was positioned so that reliable pressure data were measured for their seated position, a seat belt was used to hold the pelvis in place. The seat belt was tightened and the pelvic plate was pressed forward (Figure 4) to further insure the pelvis was held fixed.

The subject's feet were placed so that the tibia was perpendicular to the floor. The seat height was then adjusted so that the knee angle was at 105° . A shoulder support was placed in front of the subject's shoulders while the subject maintained a neutral upright posture. The shoulder support was instrumented so that the X and Z position of the shoulder pads were known. Thus, the initial position of the subject's shoulders was known. Subjects sat in five postures:

1. Neutral
2. Extension
3. Slumped 1
4. Slumped 2
5. Slumped 3

These postures represent the full range of positions for a subject in a driving posture. The three-dimensional coordinates were measured for points on the thigh, pelvis, chest and spine for each of the five postures. These data will be used to develop a model that predicts spine contour based on the position of the chest relative to the pelvis; however, for this report we will describe only the data relative to the pelvis.

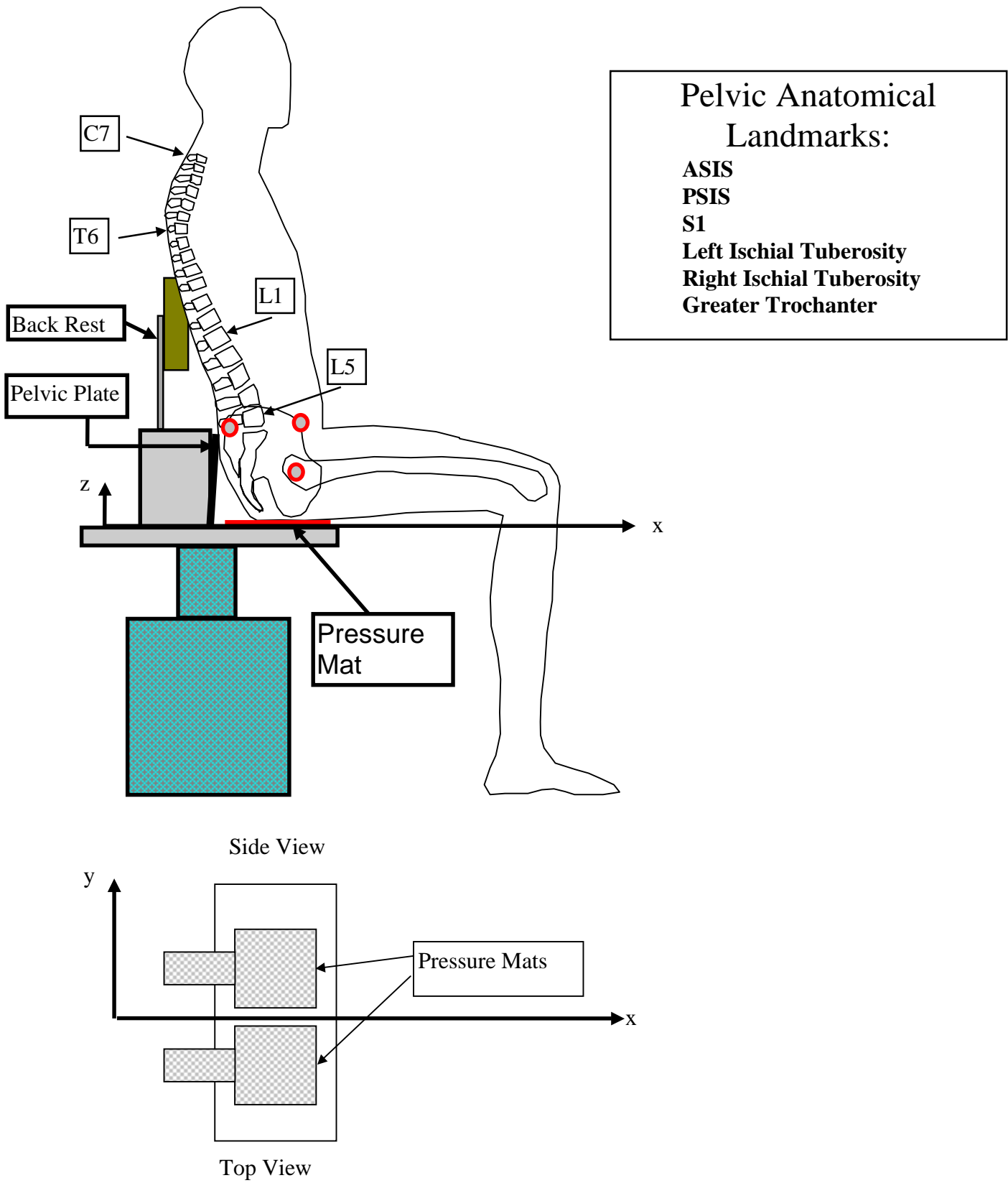


Figure 4. Position of the subject, location of pressure mats and illustration of the pelvic landmarks measured for this research.

Five points were measured on each subject's pelvis and the greater trochanter of the femur was measured to provide additional information for our error analysis of H-point. The landmarks measured (Figure 4) were:

1. Right ASIS
2. Right PSIS
3. S1
4. Left Ischial Tuberosity (from pressure mat data)
5. Right Ischial Tuberosity (from pressure mat data)
6. Greater Trochanter.

One additional point (H-point) was calculated from the measured data, using the method described in section II.A.

3. Locating the Ischial Tuberosities from Pressure Mats

In this report we describe the methods used to locate the peak pressure on a pressure mat for a subject seated on the hard surface of the SAS (spine anthropometry seat). The position of the pressure mats was measured using the CMM; thus the location of each pressure cell could be mapped back to the CMM coordinate system.

The four vertices of the pressure mat (v_1 , v_2 , v_3 and v_4) determine its position (as shown in Figure 5a). The row and column number of these four vertices are $v_1=(0,0)$, $v_2=(0,m)$, $v_3=(n,0)$, and $v_4=(n,m)$. Let (x_i, y_i, z_i) be the 3D coordinate of the vertex i . Given a point, $P(r,c)$, on the pressure mat, where r is the pressure mat row (y direction) and c is the column (x axis), the 3D coordinate of the point P is determined as follows:

$$P_x = x_1 + \frac{(x_2 - x_1) + (x_4 - x_3)}{2m} c$$

$$P_y = y_1 + \frac{(y_2 - y_1) + (y_4 - y_3)}{2n} r$$

$$P_z = z_i$$

Here, we assume that the mat lies on the xy -plane, so the z value is the same for every point on the mat.

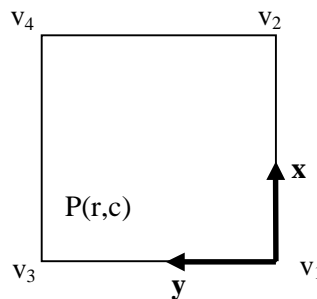


Figure 5a. Locating pressure cell P , given the coordinates of the pressure mat corners.

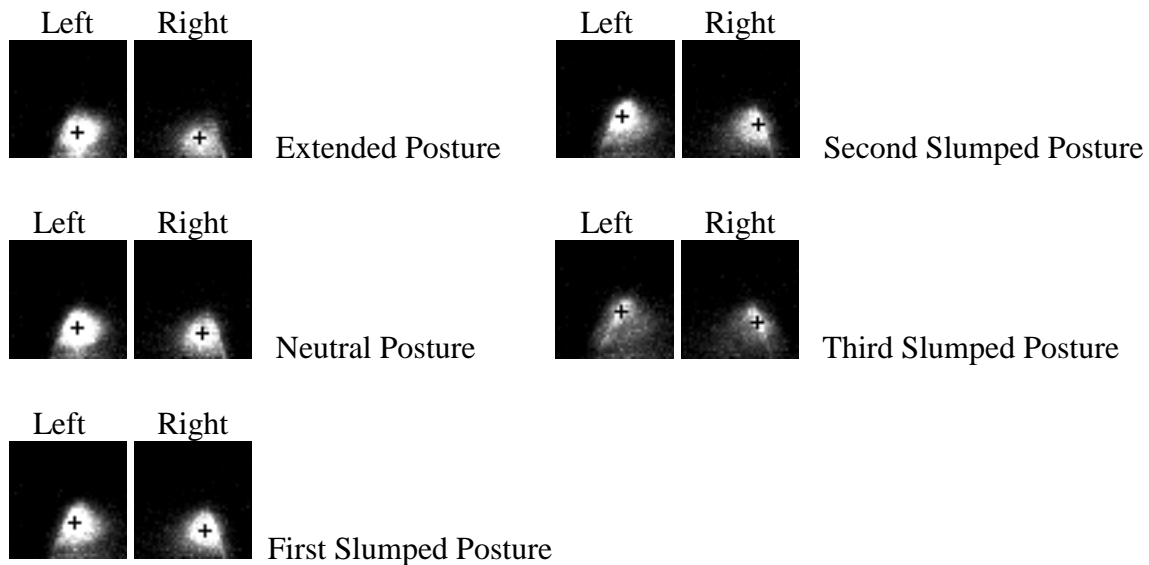


Figure 5b. Pressure maps of a subject seated in different postures. A black cross indicates the location of the pressure peaks under the ischial tuberosities.

A series of pressure mappings of a subject seated in the SAS are illustrated in Figure 5b. The black crosses illustrate the location of the pressure peak. In these illustrations the dark areas indicate low pressure and bright areas indicate high pressure.

We assume that the center of the ischial tuberosities is located at the area of peak pressure. However, inspection of the pressure images reveals (Figure 5b) that data from subjects seated on these mats have a high-pressure plateau instead of a single point that could be defined as the peak. We therefore define the peak as the centroid of the largest closed region of high-pressure values. The procedure of locating the peak is as follows:

- 1) Smooth the pressure map using a Gaussian mask to remove the effects of isolated high pressure points.
- 2) Threshold the pressure map.
- 3) After thresholding, the pressure map may have several connected components. We pick the largest component.
- 4) Locate the peak as the centroid of the largest connected component.

4. Correcting for Tissue over the ASIS

The posture of each of the 102 subjects was recorded in a seat buck using the video anthropometry system described previously (see [8] for further details). In this report we analyze the effect of tissue and clothing on measuring the ASIS. There are three sources of error involved with measuring anatomical landmarks. The first is the error involved with identifying the landmark. This error is minimized for bony landmarks such as the ASIS. Although we recognize this error exists we do not address it in this report. The second source of error is the error of the measuring equipment. The measurement error for the video anthropometry system is approximately 0.2% of the field

of view [5, 6]. The third source of error is placement of the retro-reflective target over the anatomical landmark and the movement of that target over skin and clothing. Due to the fact that the ASIS is in a sensitive and private area of the body, we place the retro-reflective target over the clothing covering that point. In the seated posture, fat and tissue often lie over the ASIS, making it more difficult to accurately place a target. In this section we describe our procedures for measuring the effect of tissue and clothing between the ASIS and a retro-reflective target overlying the ASIS.

Subjects. All 102 subjects described in section III [2] were involved in this portion of the study.

Subject Placement. Subjects were asked to sit in a seat buck [8]. The subject then adjusted seat position and steering wheel position to a comfortable location.

Target Placement. Video anthropometry measurements require retro-reflective targets be placed over anatomical points that are to be measured. A retro-reflective target, approximately 1" diameter, was placed so that the center of the target was at the center of the ASIS landmark on the XZ sagittal plane (Figure 6). An experienced technician, familiar with anatomy and ASIS location, placed the targets on the subject.

Target Measurement. The CMM was mounted in a preset location and a coordinate system was established so that the CMM coordinate system was identical to that used to calibrate the camera measurement space. The position of the ASIS was then measured with the CMM. If significant tissue was present, the tissue was moved and compressed so that the tip of the CMM was at the ASIS. Once the 3-D coordinates were recorded with the CMM, the retro-reflective target placement was double checked to insure that it was located at the projection of the ASIS on the XZ plane. Video images of the ASIS target were then captured and the three-dimensional coordinates were computed [5]. The location of the ASIS from the video anthropometry system was compared to the CMM measurement. The results are described in section III.4 of this report.

Tissue Adjustment Vector. Since great care was taken to insure that the ASIS was projected onto the XZ plane it is expected that an adjustment vector can be developed for each drive subject. This adjustment vector is expected to have a dominant, if not an exclusive, Y-axis component. The results are described in section III.4 of this report.

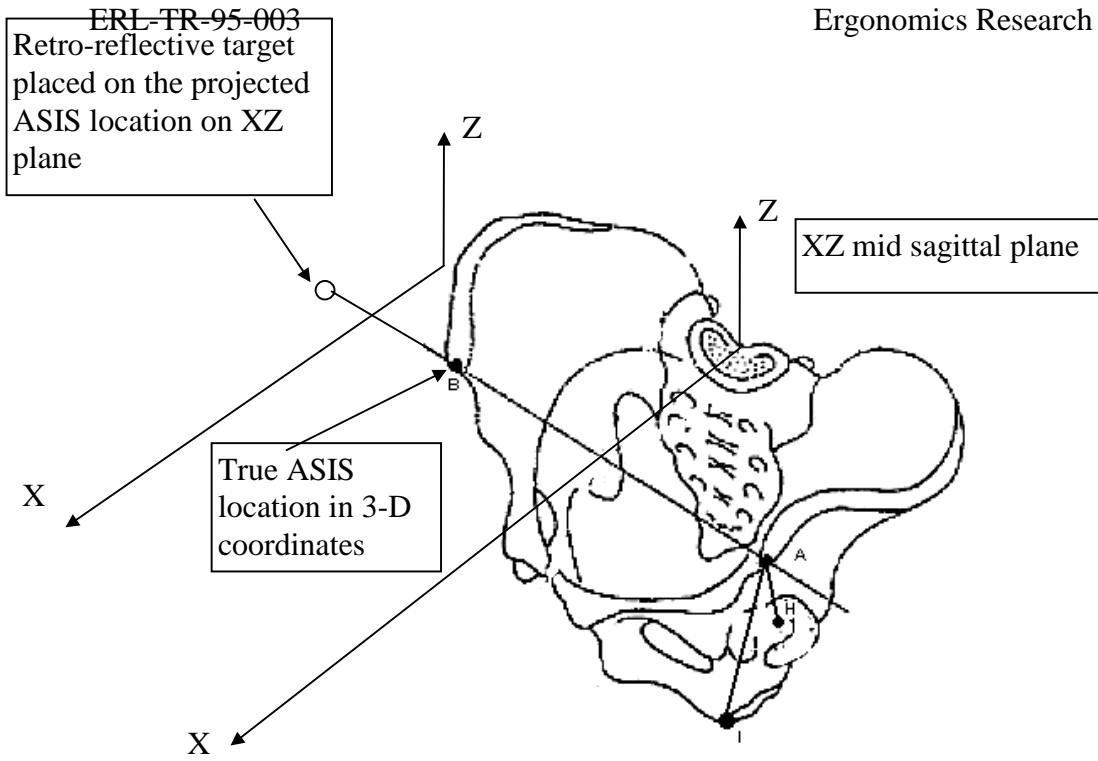


Figure 6. Projected location of the ASIS on the XZ plane.

III Results

1. Reliability of SAS Pelvic Measurements

Five postures were measured for each subject, providing a means of comparing the relative positions of each pelvic landmark. Since the exact location of the landmarks are not known, the error will be estimated from the standard deviation of the change in length of the vector between the various landmarks.

The most easily palpated landmark is the ASIS, thus the errors involving that vector are expected to be lower than vectors not containing that vector. The most difficult points to locate are the PSIS and S1, primarily due to the tissue overlying these points. Thus, it is expected that the CMM measurement errors can be described by investigating the standard deviation of the relative length change of the vector between S1 and PSIS and the vector between PSIS and ASIS.

The ischial tuberosities are measured using the pressure mats. However, the error in locating these points using this system is not known, thus we will estimate the error by investigating the standard deviation of the change in length of the vector between the two ischial tuberosities.

Analytical methods: Estimating measurement error. Given a set of repeated 3-D measurements of two points in space, \mathbf{P} , \mathbf{Q} where \mathbf{P} , \mathbf{Q} are on a rigid body that is moving in space, then one means of examining measurement errors is to determine the change in length of the vector \mathbf{r} (where $\mathbf{r} = \mathbf{P} - \mathbf{Q}$). If we denote $r = \|\mathbf{r}\|$, then for n measurements of \mathbf{P} , \mathbf{Q} , the standard deviation of r_i (where $i = 1..n$) is an estimate of the error.

If there are several subjects, each having the points \mathbf{P} , \mathbf{Q} measured, then what is the overall error in measuring the points \mathbf{P} , \mathbf{Q} for all subjects? Due to differing body sizes, the length of r varies between individuals. To overcome this problem, we investigated the change in length of the vector \mathbf{r} with respect to the average length:

$$s_i = r_i - r_{ave}$$

where r_{ave} is the average length of the vector \mathbf{r} for n measurements from one subject and s_i is the change in length relative to the average length for \mathbf{r} .

The standard deviation of the s_i values over n measurements is the same as that for r_i , but the values for s_i are independent of the subject and simply indicates measurement error, since the effect of vector length has been removed.

Estimates of errors for measuring pelvic landmarks. We will examine the standard deviation of the change in length of the following vectors (Figure 7):

s_1 = change in length of the vector from S1 to PSIS (\mathbf{r}_1) relative to the average length of that vector over five measurements for each subject.

s_2 = change in length of the vector from PSIS to ASIS (\mathbf{r}_2) relative to the average length of that vector over five measurements for each subject.

s_3 = change in length of the vector from the left ischial tuberosity to ASIS (\mathbf{r}_3) relative to the average length of that vector over five measurements for each subject.

s_4 = change in length of the vector from the right ischial tuberosity to ASIS (r_4) relative to the average length of that vector over five measurements for each subject.

s_5 = change in length of the vector from the left to the right ischial tuberosity (r_5) relative to the average length of that vector over five measurements for each subject.

s_θ = change in the angle between the PSIS-ASIS-ischial tuberosity relative to the average angle between those points over five measurements for each subject (note: the angle is the projected angle between those points on the XZ plane (sagittal plane) as defined in the coordinate system for the SAS).

The analysis only includes the results from 34 subjects. Due to a change in protocol and technical difficulties a complete set of five pelvic measurements was only obtained on 34 subjects.

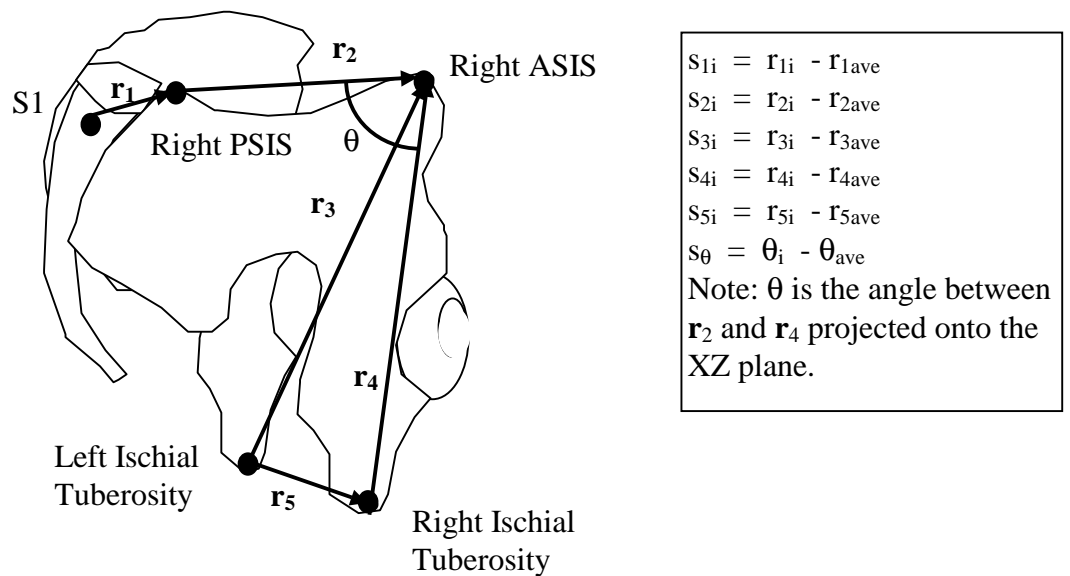


Figure 7. Length and angle changes used to estimate measurement errors.

Vector Name	Vector Description	Standard Deviation (mm) (for 34 subjects, 5 postures each)
s ₁	Length change from average S1-PSIS vector	6.11
s ₂	Length change from average PSIS-ASIS vector	4.51
s ₃	Length change from average left ischial tuberosity -ASIS vector	3.11
s ₄	Length change from average right ischial tuberosity -ASIS vector	3.45
s ₅	Length change from average left to right ischial tuberosity vector	3.63
s ₆	Angle change from the projected angle of PSIS-ASIS- ischial tuberosity vectors onto XZ plane.	3.06 ^o

Table 3. Error estimates for measuring anatomical landmarks on the human pelvis.

2. Pelvic Dimensions

Subject pelvic dimensions were compared to their equivalents in the database [1]. Specifically, the PSIS-ASIS distance, the left-right ischial tuberosity distance and the left-right ASIS distances are compared (Table 4). The dimensions were calculated as the Euclidean distance between landmarks. #399 was used for the ischial tuberosity.

Vector	Sex	Minimum (mm)		Maximum (mm)		Average (mm)		Std Dev (mm)	
		Present Study	Reynolds et al						
ASIS to Isch Tub	Male	181.2	144.2	224.4	189.7	200.9	168.8	9.9	8.9
	Female	153.9	133.9	212.9	180.0	182.4	156.5	11.2	8.9
L ASIS to R ASIS	Male	194.2	187.3	297.7	265.1	237.7	227.1	18.4	16.7
	Female	169.0	162.0	278.1	274.1	227.6	223.7	21.2	21.1
L Isch Tub (408) to R Isch Tub	Male	61.1	98.1	131.8	153.9	106.3	120.3	11.2	11.3
	Female	85.1	96.6	149.4	158.5	123.8	135.5	12.7	12.6
L Isch Tub (399) to R Isch Tub	Male	61.1	58.2	131.8	109.5	106.3	79.5	11.2	12.0
	Female	85.1	60.8	149.4	124.5	123.8	97.5	12.7	11.7
R PSIS to R ASIS	Male	128.7	138.1	208.8	174.6	170.3	158.0	13.2	8.7
	Female	124.7	130.7	192.6	169.9	163.6	149.4	12.4	8.5

Table 4. Distances between pelvic landmarks, comparing the present study to a database of skeletal pelvis. The skeletal pelvis are described in Reynolds, *et al* [1].

Since foam was placed over the mats, the distance from the ischial tuberosity to the ASIS was calculated after adjusting for foam thickness. Foam thickness was measured using a skinfold caliper (Holtain, Ltd, Crymych, U.K.) to apply a known pressure while simultaneously measuring thickness. The calipers apply 10 gms/mm² and are accurate to 0.1mm. The foam thickness was calculated after the caliper pressure was applied for at least 1 min., to minimize the effect of creep in the foam thickness measurement. The pressure applied by the calipers is similar to the pressure under the ischial tuberosities and thus the foam thickness measured with this technique will be close to that of the foam as it was compressed by the subject.

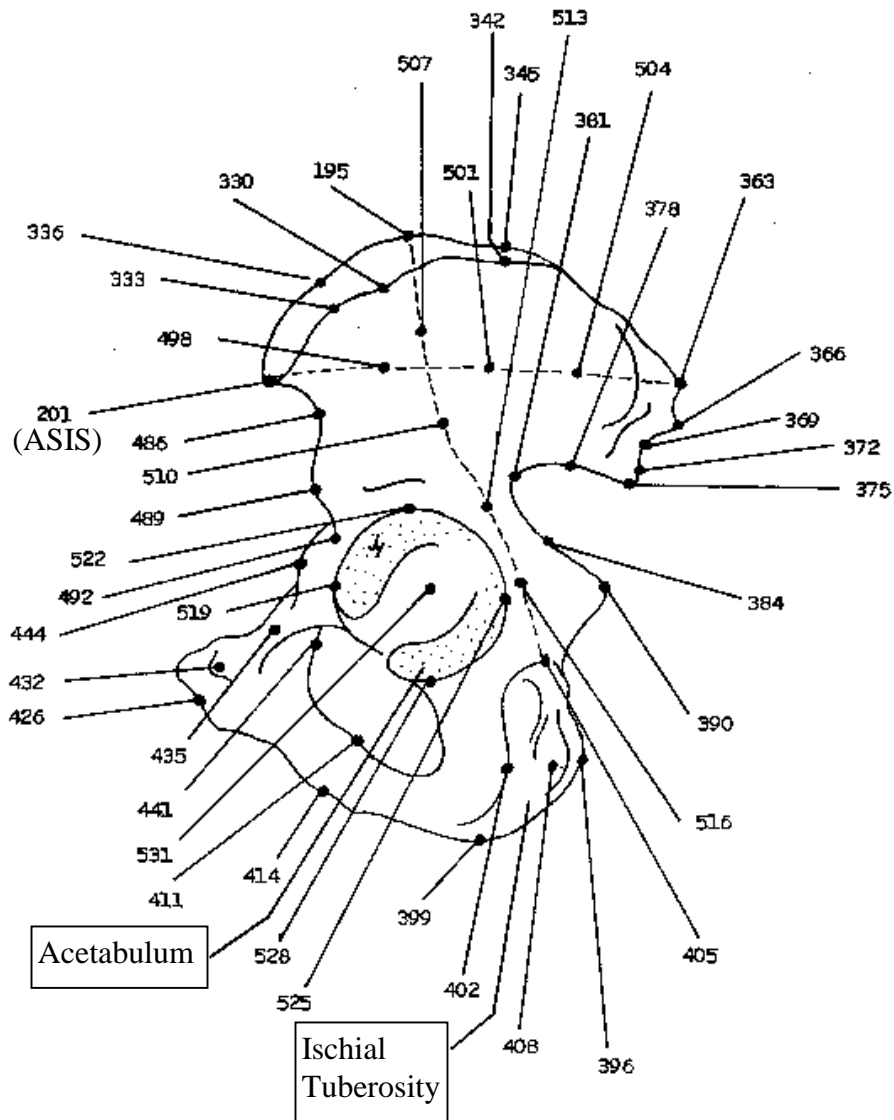


Figure 8. Pelvic landmarks measured in the pelvis database. The pelvis database is described in Reynolds, *et al* [1].

3. Pelvic motion between spinal postures

The motion of the pelvis was restricted by holding the subject's pelvis to the seat using a seatbelt and by pressing the pelvis into the seatbelt using the pelvic plate (Figure 4). The purpose of the experiment was to determine the change in shape of the spine based on chest position relative to the pelvis. In order to reduce data collection variability, we fixed the pelvis and changed chest position. The purpose of this section is to determine the extent to which the pelvis was held fixed.

The motion of the ASIS point and the peak pressure (i.e., ischial tuberosity) point were calculated for all five measurements. The data described here is from a subset of 34 subjects having all five measurements of all points uncorrupted. The primary reason for loss of pressure mat data was due to a decrease in the amount of pressure applied to the pressure mats, reducing the ability of the mats to discern the location of the ischial tuberosities. This decrease in pressure occurred because subjects rested upper body weight against a chest support for the three slumped postures.

Landmark	Description	Motion (Std Dev of Position Change from Average)	
R ASIS	Position change from average location of the R ASIS for 5 measurements for each subject.	X Std Dev 5.15 mm	Z Std Dev 5.87mm
R Ischial Tuberosity	Position change from average location of the R Ischial Tub. for 5 measurements for each subject.	X Std Dev 4.77mm	Y Std Dev 2.39mm
L Ischial Tuberosity	Position change from average location of the L Ischial Tub. for 5 measurements for each subject.	X Std Dev 5.07mm	Y Std Dev 2.03mm
ASIS-Ischial Tuberosity Angle	Angle change from the average angle from vertical for the RASIS - R Ischial Tube vector for 5 measurements for each subject.	Angle = 2.99°	

Table 5. Motion of pelvic landmarks for five spinal postures. Motion was determined from the standard deviation from the average position of each landmark.

The ischial tuberosity motion was studied in more detail to determine the extent to which there are differences between the five postures. The motions of each posture relative to the initial (neutral) posture are summarized in Table 6. The largest differences were between the two extreme positions. Between the extended posture and neutral posture the ischial tuberosity moved an average of +4.4mm (anterior) and for the final slumped posture it moved an average of -4.5mm (posterior) relative to the neutral position. An ANOVA was performed to determine the significance of these differences. The motions between the extended posture and the neutral posture were significantly different as were the motions between the full slumped posture and neutral ($p < .05$).

Although there were statistically significant motions of the ischial tuberosity, the motion of the pelvis as a whole was limited. The standard deviation of the angle change between the ASIS-ITCH vector from vertical was 2.99° , indicating the posture of the pelvis was held relatively constant.

Position Change	Average Ischial Tuberosity Movement in the X direction (mm)	Std Dev (mm)
Neutral to Extension	4.4	3.5
Neutral to Slump 1	-1.1	3.9
Neutral to Slump 2	-3.8	6.7
Neutral to Slump 3	-4.5	9.3

Table 6. Average change in the position of the ischial tuberosity relative to the initial (neutral) posture.

4. ASIS Tissue Correction Vector

In the automobile there are only two landmarks on the pelvis that can be measured using non-invasive means. The ASIS can be measured using video anthropometry [5, 6] and the ischial tuberosities can be measured using a pressure mat system. The error in the video anthropometric system [5] is approximately 1 part per 500 or 0.2 percent of the field of view. The experimental error in the video anthropometric system, however, is affected by clothing and tissue.

The extent to which tissue and clothing exaggerate the position of the ASIS, however, is not known. In the seated posture, a significant amount of tissue may overlie this point. In addition, clothing “bunches up” to cause an erroneous measurement. In order to reduce these errors, the ASIS target was placed on a point that represents the projection of ASIS on the XZ (sagittal) plane as shown in Figure 6. The error in ASIS position as measured by the video anthropometric system was compared to a CMM measurement of the ASIS anatomical landmark as palpated by a trained technician. The CMM measurement was made with the tissue and clothing compressed as close to the skeletal landmark as possible, thus, the difference between the two measurements can be used to calculate a tissue correction vector. Both measurements were used for the same posture for subjects sitting in the seat buck [5]. The differences in these two measurements are summarized in Table 7. The tissue correction vectors have a predominant difference in the X and Y directions, but almost no difference (on average) in the Z direction.

	X	Y	Z
Average Difference (mm)	-11.9	+8.8	- 0.8
Standard Dev (mm)	10.8	10.1	8.1

Table 7. Average and standard deviation of the tissue correction vector.

A linear regression of weight vs height for all subjects showed that $\text{Weight(Kg)} = 0.98 \text{ Height(cm)} - 97.7$ ($r^2 = 0.63$). To calculate a true to estimated weight ratio, the subject's true weight was divided by their estimated weight. The positive correlation ($r^2 = 0.17$) between the true weight/estimated weight (correction magnitude in mm = $60.5(\text{weight/estimated weight}) - 44.3$) and the ASIS correction vector magnitude indicates that at least part of this magnitude is due to the tissue overlying that point (Figure 9).

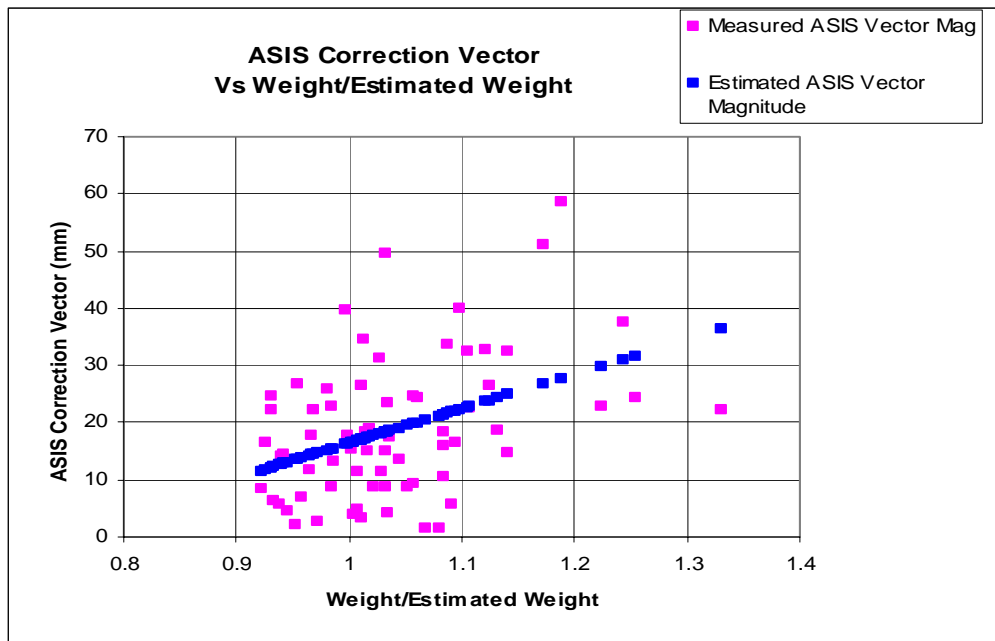


Figure 9. ASIS Correction vector magnitude versus subject weight divided by the estimated weight for their height.

Since there is a correlation between the correction magnitude and weight/estimated weight, a correction vector was developed for each subject. The average Z error was near zero and the Z standard deviation was only slightly larger than the measurement error for the system. Thus, the correction vector was limited to the XY plane only. The correction vector was set at 75% of the vector length in the XY plane for all vectors exceeding 10mm in magnitude. The reason for choosing this correction method was to reduce any "over-corrections" and to eliminate the need for any corrections where the vector magnitude did not exceed the measurement error of the system. A table of subject ID and correction vectors is listed in Appendix A.

5. Calculating H-point

H-point was estimated using the method described in Section IIA. of this report. The ischial tuberosity location was adjusted to account for tissue thickness [9] (see Appendix C). The tissue between the ischium and seat was assumed to be 13mm and the tissue between the skin and ASIS was assumed to be 5mm. The results were compared to the measured location of the greater trochanter and are shown in Figure 10. The greater trochanter is higher ($z = 17.6 \pm 12.5\text{mm}$) and more posterior ($x=0.6 \pm 11.6\text{mm}$) than the estimated hip joint center and 101.4 \pm 11.6mm lateral (y axis) to the hip joint center. The coordinates for H-point are listed in Appendix B for all subjects, along with the coordinates of all 5 measured pelvic landmarks.

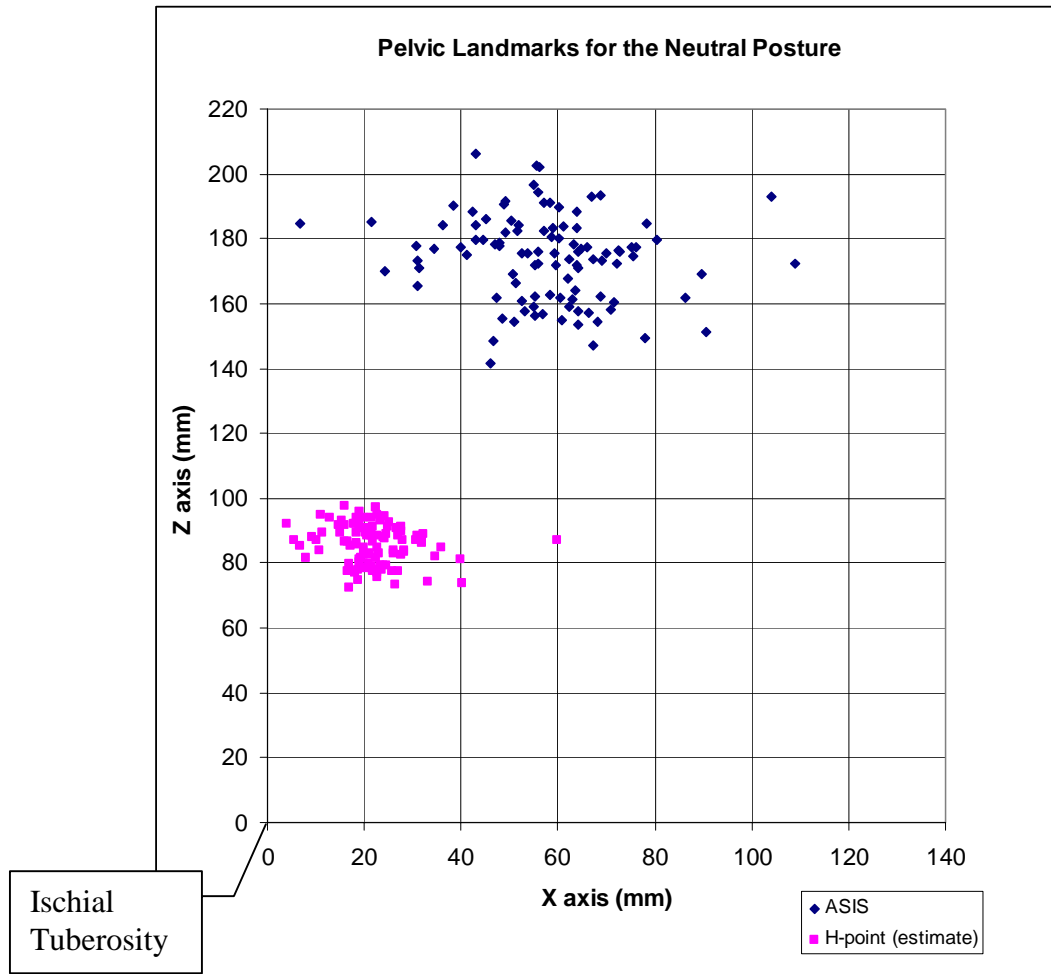


Figure 10. Location of ASIS, Ischial Tuberosity (point 0,0) and the estimated location of H-point. Only the X-Z projection (sagittal plane) is illustrated.

6. Testing the Analytical Methods

In our experiments with human subjects, the ischial tuberosity points were detected based on locating the peak pressure from pressure mats. However, since the ischial tuberosity is a curved surface approximately 7-8 cm in length, we do not know

exactly which point on the ischial tuberosity the peak pressure corresponds to. Since locating the ischial tuberosity is a key component of our technique for calculating H-point, we investigated the effect of using different points on the ischial tuberosity and the corresponding error in locating H-point. In Section IIA, point #408 of the Reynolds, *et al* [1] database was used. This point is the most posterior point of the ischial tuberosity, and it lies midway along the complete surface of the ischial tuberosity. We used point #399 (the most anterior point of the ischial tuberosity in the data base) and an estimated mid point (the mid-point between points #399 and #408) and calculated H-point using the method described in Section IIA. This provides a means of determining the accuracy of the method as well as the robustness of the approach in the cases where the inputs are not the exact points used in developing the regression equations. The error was estimated using the Euclidean distance between the calculated hip joint point and the true 3D coordinates of the hip joint point from the database. The results are summarized in Table 8.

Gender	Input type	Mean Error (mm)	Std. Dev.(mm)
Male	Posterior (408)	6.98	3.04
Male	Anterior (399)	16.68	4.76
Male	Middle	9.11	3.85
Female	Posterior (408)	8.39	3.29
Female	Anterior (399)	13.14	4.36
Female	Middle	7.22	3.11

Table 8. Mean and standard deviation of the error for locating H-point.

IV. Discussion

The error estimates for measuring anatomical landmarks on the human pelvis (Table 3) show that the largest errors occur between S1 and the PSIS. These landmarks are difficult to identify on most subjects due to the large amount of tissue overlying these points. The standard deviations between the ischial tuberosities and the right ASIS are the smallest, indicating that these measurements are the most reliable. To clarify the magnitude of these differences, the pressure mats used to locate the ischial tuberosities have a distance of 2.5mm between sensor cells. This inter-sensor distance is just slightly smaller than the error estimate of 3.63 mm, standard deviation in vector length between the right and left ischial tuberosities (s_5 in Table 3). Thus, the pressure mat is as reliable as human palpation for locating a bony anatomical landmark.

In Table 4 the pelvic dimensions for the 102 subjects in the current study are compared to the dimensions from the pelvic database [1]. The PSIS-ASIS length is larger for the current study than the equivalent length in the database. This difference is expected because there is considerable tissue overlying ASIS and PSIS, which adds to the vector length compared to a similar measurement taken over dry bone.

The inter-ischial tuberosity distance was found to be 106.3 mm (males) and 123.8 mm (females). In the Reynolds *et al* data base there are two points that were measured on

the ischial tuberosity that correspond to the ischial tuberosity measurements in this study, and these points are #399 and #408 in Figure 8. The more anterior point, #399, has a mean distance from its contra-lateral point of 79.5mm (males) and 97.5mm (females). Using #408 the inter-ischial tuberosity distance is 120.3mm (males) and 135.5mm (females). The inter-ischial tuberosity distance measured in this study lies between these two; thus the point being measured on the subjects' pelvis lies between the anterior of the ischial tuberosity, #399, and the posterior point of the ischial tuberosity, #408.

There is an average difference between the current study and the pelvic data base for the distance between the ischial tuberosity and the ASIS of 32.1mm for males and 25.9mm for females (Table 4). For males this distance averaged 200.9mm (compared to 168.8mm in the pelvic data base) and 182.4mm for females (compared to 156.5mm in the pelvic data base). Tissue thickness under the ischial tuberosities accounts for 10-15mm of the differences [9] (see Appendix C) and palpation error on living subjects accounts for the remainder. For the PSIS-ASIS vector length the errors are on the order of 12-13mm, an acceptable error range considering tissue deposits and palpation errors.

An analysis of the ischial tuberosity motion over the five postures (Table 5) shows that the ischial tuberosity slid rearward and the pelvis rolled forward as the subjects slumped forward and rested their chest on the chest support. It is not likely that the centroid of the pressure mat corresponded to the same point on the ischial tuberosity for all five measurements. This raises the question of the effect an erroneous point on the ischial tuberosity has on the estimated location of H-point. An analysis of the pelvic database reveals that the regression model is fairly robust and that the error in calculating H-point is minimal (Table 8).

The H-point calculation method of section II was tested using the data from the pelvic database [1]. We conducted three tests to determine the ability of the regression equations to accurately predict H-point. In the first test, the 3D coordinates of the right ASIS point and the posterior point of the left and right ischial tuberosity were used as input. In the second test, we used the right ASIS point and the left and right anterior point of the ischial tuberosity points. In the last test, we used the right ASIS point and the left and right midpoints between posterior and anterior points of the respective ischial tuberosities. The same regression lines developed in the previous sections were used and the mean of α in Table 2 was used to compute the hip joint point.

The results (Table 8) show that our method is accurate as well as robust. The H-point calculated using mid points of the ischial tuberosities are fairly comparable with the posterior points; and, for the females, it is even better than the posterior points. We believe this is because the point **H** is not exactly coplanar with the points **A**, **I_L** and **I_R**, it is slightly forward, near the plane determined by the point **A** and two middle points. These results are important since, in the seated posture, subjects most likely are seated at some point between the anterior and posterior aspects of the ischial tuberosities.

Other researchers have described various procedures for locating the hip joint. Andraicchi, *et al* [10] defined the hip joint to be 1.5cm distal to the midpoint of a line connecting the ASIS to the pubic symphysis. Tylkowski, *et al* [11] described the hip center in terms of a percentage of the inter-ASIS distance, with H-point located 11% medial to the ASIS, 12% inferior to the ASIS and 21% posterior to the ASIS. Bell, *et al* [12] described three methods for locating the hip joint center and used bi-planar

radiographs to determine their accuracy. They reported that a kinematic analysis of locating the hip center had an average error of 37.9mm, with errors ranging from 14mm to 63mm. The method described by Andracchi [10] had similar error ranges with an average error of 36.1mm and a range of 14.8mm to 44.0mm. The method described by Tylkowski [11] had average errors of 19mm and an error range of 4.9mm to 34.9mm. Others have modified the work of Tylkowski and co-workers. Manary, *et al* [13] used a modification of Tylkowski's method [12] to locate H-point and Seidel, *et al* [14] further improved this approach by examining 35 female and 30 male cadavers. They reported H-point to be located 14% of pelvic width medial to the ASIS, 34% of pelvic depth posterior and 79% of pelvic height inferior to the ASIS.

The disadvantage of the above methods for locating H-point is the need to locate the pubic symphysis. This is a difficult area of the body to measure due to clothing and tissue overlying the area. In addition, many subjects would not feel comfortable with measurements taken at that area. The advantage of the method described in IIA of this report is the ease with which it can be adapted to the seated posture and the accuracy and robustness of the technique.

References

1. Reynolds, C. Snow and J. Young, *Spatial geometry of the human pelvis*, FAA-AM-82-9}, 1982.
2. Comas J, *Manual of Physical Anthropology*, Bannerstone house, Springfield, IL, 1957.
3. Francis, *The Human Pelvis*, C.V. Mosby company, St. Louis, 1952.
4. Rosner B. *Fundamentals of Biostatistics*, Duxbury Press, Boston MA, 1982.
5. Stockman G, Chen J, Moore M, Cui Y, Reynolds H. Computing body posture of automobile drivers using multiple cameras. Paper submitted for publication, 1995
6. Reynolds HM, Majumder A, Rayes K, Eppler M, Neal D, Moeggenberg B, Dinnan B. The Initial Position and Postural Attitudes of Driver Occupants. Final Report. February 28, 1994. Inland Fisher Guide Division, General Motors Corporation.
7. Eppler M, Bolster V, Reynolds H. The Initial Position and Postural Attitudes of Driver Occupants. Anthropometry. ERL-TR-95-002, Ergonomics Research Laboratory, Michigan State University, 1995.
8. Reynolds HM, Brodeur R, Eppler M, Neal D, Rayes K, Kerr R, Stockman G. The Initial Position and Postural Attitudes of Driver Occupants. Experimental Protocol. ERL-TR-95-001, Ergonomics Research Laboratory, Michigan State University, 1995.
9. Daniels, Stan, Personal communication.
10. Andriacchi TP, Andersson GBJ, Fermier RW, Stern D, Galante JO, A study of lower-limb mechanics during stair climbing. *J Bone and Joint Surgery*, 62A:749-757.
11. Tylkowski CM, Simon SR, Mansour JM, Internal rotation gait in spastic cerebral palsy in the hip. Proceedings of the 10th open scientific meeting of the hip society (Nelson JP, ed), pp 89-125, Mosby, St. Louis.
12. Bell AL, Pedersen DR, Brand RA. A comparison of the accuracy of several hip center location prediction methods. *J Biomechanics*, 23(6):617-621, 1990.
13. Manary MA, Schneider LW, Flannagan CC, Eby BH. Evaluation of the SAE J826 3-D manikin measures of driver positioning and posture. SAE 941048, 1994.
14. Seidel GK, Marchind DM, Dijkers M, Soutas-Little RW, Hip joint center location from palpable bony landmarks: a cadaver study. *J Biomechanics*, 28(8):995-998, 1995.

Appendix A

ASIS Tissue Correction Vector

This table lists the correction vectors for adjusting for tissue thickness over the ASIS. Delta x,y,z are the differences between the video anthropometric measurement of the ASIS target and the CMM measurement of the bony landmark. The correction vector is zero for vectors having a magnitude of less than 10mm and 0.75 of the x, y coordinates for all other vectors. The correction vector is from the bone to the target.

Sub ID	Sex	Delta x	Delta y	Delta z	Mag	ASIS Correction Vector	
						X	Y
1	F	1.14	3.8	-0.46	3.967316	0	0
2	F	-1.24	-8.57	4.36	8.659244	0	0
3	F					0	0
4	F	27.4	-25.58	22.56	37.48462	20.55	-19.185
5	F					0	0
6	F	19.83	-14.78	0.47	24.73211	14.8725	-11.085
7	F	0.38	-4.48	2.79	4.496087	0	0
8	F	18.19	-13.85	-1.95	22.8626	13.6425	-10.3875
9	F	27.12	-17.94	10.29	32.51673	20.34	-13.455
10	F					0	0
11	F	43.01	-39.68	9.32	58.51805	32.2575	-29.76
12	F	9.64	-9.45	-1.14	13.49934	7.23	-7.0875
13	F	29.42	-14.58	12.62	32.83463	22.065	-10.935
14	F	12.03	0.93	-8.87	12.06589	9.0225	0.6975
15	F	0.88	-14.09	-0.51	14.11745	0.66	-10.5675
16	F	6.45	-0.47	-1.02	6.467101	0	0
17	F	0.47	-0.09	0.07	0.478539	0	0
18	F					0	0
19	F	20.33	-9.2	-2.35	22.31477	15.2475	-6.9
20	F	3.87	4.26	-7.91	5.755389	0	0
21	F	2.88	-2.55	-2.43	3.846674	0	0
22	F	1.58	0.26	-5.44	1.60125	0	0
23	F	7.85	-5.32	0.25	9.482874	0	0
24	F	21.31	-15.66	4.79	26.44526	15.9825	-11.745
25	F	8.7	-0.05	-7	8.700144	0	0
26	F	26.03	-22.62	11.67	34.48515	19.5225	-16.965
27	F	12.3	-9.41	-1.2	15.48671	9.225	-7.0575
28	F	22.42	-9.14	-3.96	24.21148	16.815	-6.855
29	F	-4.47	-5.26	0.89	6.902789	0	0
30	F	12.65	-2.98	-7.74	12.99626	9.4875	-2.235
						ASIS Correction Vector	

Sub ID	Sex	Delta x	Delta y	Delta z	Mag	X	Y
31	F	14.25	-17.09	4.97	22.25153	10.6875	-12.8175
32	F	3.98	-13.86	-8.22	14.42012	2.985	-10.395
33	F	5.35	-4.51	-3.17	6.997328	0	0
34	F	9.54	-8.48	-4.57	12.76409	7.155	-6.36
35	F	22.09	-4.86	1.72	22.6183	16.5675	-3.645
36	F	1.84	-1.19	-10.83	2.191278	0	0
37	F	14.33	-19.98	16.17	24.58758	10.7475	-14.985
38	F	26.73	2.29	-3.51	26.82791	20.0475	1.7175
39	F	2.04	-8.48	-5.2	8.721926	0	0
40	F	9.17	-1.07	7.6	9.232215	0	0
41	F	14.84	-5.62	9.36	15.86852	11.13	-4.215
42	F	23.51	-10.99	7.5	25.95188	17.6325	-8.2425
43	F	17.66	-16.88	3.02	24.4297	13.245	-12.66
44	F	12.37	-8.39	11.93	14.94687	9.2775	-6.2925
45	F	29.07	-27.01	18.91	39.68129	21.8025	-20.2575
46	F	31.02	-38.82	19.85	49.69138	23.265	-29.115
47	F	10.56	-4.3	-1.1	11.40191	7.92	-3.225
48	F	21.03	-6.94	12.79	22.14553	15.7725	-5.205
49	F	21.97	-16.32	16.55	27.36829	16.4775	-12.24
50	F	8.63	-10.19	-0.58	13.35339	6.4725	-7.6425
51	M	3.7	-2.9	-1.14	4.701064	0	0
52	M					0	0
53	M	-4.39	-6.06	4.47	7.483027	0	0
54	M	30.5	-7.32	-14.78	31.3661	22.875	-5.49
55	M	0.93	1.94	-1.84	2.151395	0	0
56	M					0	0
57	M	30.28	-28.52	19.04	41.5965	22.71	-21.39
58	M	2.6	8.28	-6.39	8.678617	0	0
59	M						
60	M	8.52	-1.68	-0.23	8.684054	0	0
61	M	-1.09	-1.95	0.52	2.233965	0	0
62	M	27.28	-17.82	5.48	32.58452	20.46	-13.365
63	M	18.38	-18.81	-1.61	26.29906	13.785	-14.1075
64	M	8.66	-14.99	9.09	17.31172	6.495	-11.2425
65	M	-7.66	-4.36	-5.57	8.813921	0	0
66	M	3.2	-11.38	-1.83	11.82135	2.4	-8.535
67	M					0	0
68	M	9.7	-20.8	-5.23	22.9506	7.275	-15.6
69	M					0	0
70	M	-0.34	-11.39	1.89	11.39507	-0.255	-8.5425
						ASIS Correction Vector	
Sub ID	Sex	Delta x	Delta y	Delta z	Mag	X	Y
71	M	17.14	4.6	-11.13	17.74654	12.855	3.45

72	M	0.45	-1.44	-8.34	1.508675	0	0
73	M					0	0
74	M	1.59	-2.19	-0.75	2.706326	0	0
75	M					0	0
76	M	4.37	-18.05	2.92	18.57147	3.2775	-13.5375
77	M	13.04	1.3	0.38	13.10464	9.78	0.975
78	M	15.31	-6.18	-0.85	16.51025	11.4825	-4.635
79	M	-7.84	-15.94	1.51	17.7637	-5.88	-11.955
80	M	2.03	2.57	-3.29	3.275027	0	0
81	M	11.49	-14.36	5.87	18.39102	8.6175	-10.77
82	M	7.28	-12.76	-3.67	14.69068	5.46	-9.57
83	M	35.01	-37.35	13.71	51.19299	26.2575	-28.0125
84	M						
85	M	2.62	-10.96	2.12	11.26881	1.965	-8.22
86	M	12.98	7.47	-3.24	14.97602	9.735	5.6025
87	M	12.19	-31.41	3.19	33.69249	9.1425	-23.5575
88	M	10.7	-10.78	0.52	15.18876	8.025	-8.085
89	M	2.84	-4.79	-14.96	5.568635	0	0
90	M	22.45	-6.39	-16.97	23.34169	16.8375	-4.7925
91	M	8.71	-5.71	-2.19	10.41481	6.5325	-4.2825
92	M	7.62	3.76	-2.66	8.497176	0	0
93	M	-4.2	-0.54	-2.36	4.234572	0	0
94	M	9.72	9.22	-8.94	13.39727	7.29	6.915
95	M	16.43	0.34	3.06	16.43352	12.3225	0.255
96	M	6.09	-2.02	-6.78	6.416268	0	0
97	M						
98	M	36.02	-17.05	-4.28	39.85151	27.015	-12.7875
99	M	16.54	-7.71	-11.59	18.24872	12.405	-5.7825
100	M	17.75	-6.27	2.78	18.82486	13.3125	-4.7025
101	M	4.98	2.4	5.18	5.528146	0	0
102	M	12.6	-4.1	12.77	13.25028	9.45	-3.075

Appendix B

Pelvis Coordinates for Subjects Seated in a Neutral Posture

This appendix lists the subjects' sex and the 3-D coordinates of the right ASIS, the left and right ischial tuberosities (L IT and R IT), the location of the mid-point of the greater trochanter and the estimated location of the hip joint center (H-point).

Subject	Sex	ASIS X	ASIS Y	ASIS Z	L IT X	L IT Y	L IT Z	R IT X	R IT Y	R IT Z	GT X	GT Y	GT Z	H x	H y	H z
1	F	543.3	-113.8	167.62	466.84	83.6	12.94	483.56	-50.86	12.94	497.34	-185.1	96.02	31.1222	-17.264	63.9413
2	F	533.86	-121.6	172.84	461.84	58.6	13.84	481.06	-63.36	13.84	489.36	-177.1	96.44	28.9831	-15.141	65.5848
3	F	536.1	-109.4	186.62	469.34	51.1	12.94	468.56	-63.36	12.94	476.5	-179.8	102.28	25.7877	-8.6881	69.9218
4	F	541.88	-122.1	205.96	471.84	56.1	12.94	403.56	-80.86	12.94	508.62	-205.9	128.4	25.7153	-4.1563	74.0208
5	F	553.42	-106.7	163.98	469.34	53.6	12.94	456.06	-63.36	12.94	490.98	-181.3	87.76	33.6644	-8.6235	60.682
6	F	534.24	-131.7	175.14	474.34	41.1	12.94	483.56	-58.36	12.94	497.82	-187.9	100.46	23.6003	-21.203	67.1979
7	F	538.62	-108.4	177.24	474.34	56.1	12.94	476.06	-73.36	12.94	481.86	-184.1	101.34	24.9511	-5.0736	66.4865
8	F	556.62	-116.6	190.14	479.34	76.1	12.94	483.56	-65.86	12.94	494.2	-197	99.38	30.2027	-9.968	71.0702
9	F	538.88	-89.74	171.78	481.84	73.6	12.94	486.06	-38.36	12.94	486.46	-161.4	90.02	22.2373	-12.663	65.4642
10	F	516.92	-118.3	223.38	466.84	81.1	17.24	481.06	-63.36	17.24	494.54	-167.3	124.82	18.0471	-9.8511	81.8605
11	F	537.34	-95.86	171.04	464.34	76.1	12.94	468.56	-45.86	12.94	504.08	-161.3	118.9	29.1521	-11.576	64.5798
12	F	533.2	-109	180.12	469.34	48.6	18.34	476.06	-68.36	18.34	488.48	-174.1	110	24.9988	-7.7339	65.9922
13	F	546.62	-89.98	184.6	479.34	61.1	12.94	486.06	-60.86	12.94	497.92	-186.7	99.2	25.9201	-1.9172	68.7937
14	F	521.12	-104.7	171.5	464.34	76.1	17.24	476.06	-45.86	17.24	485.46	-148.7	104.52	22.4157	-16.329	64.2541
15	F	529.72	-113.7	192.78	489.34	71.1	12.94	481.06	-60.86	12.94	497.44	-177.9	105.12	14.355	-11.508	72.8404
16	F	527.52	-103.1	164.24	459.34	73.6	17.24	461.06	-63.36	17.24	481.48	-167.3	98.96	27.4021	-8.469	60.5122
17	F	491.76	-84.36	162.54	446.84	63.6	13.94	443.56	-45.86	13.94	471.96	-132.2	92.32	17.0484	-8.5245	61.7788
18	F	547.8	-110.8	175.1	474.34	51.1	12.94	483.56	-58.36	12.94	498.04	-177.2	115.06	29.2774	-12.257	66.207
19	F	543.04	-91.34	168.86	474.34	86.1	15.24	483.56	-58.36	15.24	491	-158.2	93.26	27.3531	-5.083	62.8496
20	F	541.86	-117.7	173	474.34	78.6	15.54	481.06	-53.36	15.54	491	-173.7	102.62	27.0106	-17.785	65.0108
21	F	551.3	-112	189.24	479.34	61.1	12.94	478.56	-70.86	12.94	488	-184.4	99.58	27.8103	-6.2735	70.4534
22	F	533.38	-105.8	170.8	476.84	68.6	12.94	483.56	-60.86	12.94	460.98	-178.4	135.64	22.015	-10.141	65.0306

23	F	539.34	-105.6	193.1	469.34	71.1	17.24	481.06	-78.36	17.24	496.96	-168.5	113.92	26.9322	-0.7497	70.1788
24	F	539.84	-129.1	189.06	481.84	38.6	12.94	486.06	-70.86	12.94	512.32	-187.7	124.4	22.1559	-13.738	71.5657
25	F	507.38	-111.3	180.84	471.84	61.1	15.24	481.06	-58.36	15.24	477.62	-157.1	110.58	12.5726	-13.186	68.4229
26	F	526.74	-93.26	174.5	461.84	81.1	12.94	466.06	-43.36	12.94	482.96	-154.9	107.96	25.536	-11.519	66.091
27	F	536.82	-121.1	186.4	469.34	66.1	15.24	476.06	-55.86	15.24	502.18	-182.1	111.78	26.4841	-16.774	69.8352
28	F	541.62	-112.5	183.54	489.34	86.1	17.24	491.06	-60.86	17.24	489.02	-178.3	110.18	19.8972	-12.159	68.1162
29	F	507.08	-119	193.6	464.34	86.1	13.94	463.56	-45.86	13.94	482.8	-172.4	111.46	15.5428	-19.679	73.5066
30	F	517.64	-109.3	155.68	469.34	41.1	13.94	473.56	-68.36	13.94	481.76	-161.2	100.98	18.8878	-10.267	59.5983
31	F	519.12	-101.9	185.42	404.34	28.6	12.94	416.06	-55.86	12.94	489.54	-167.3	116.92	45.7405	-6.9164	67.9968
32	F	508.3	-110.6	191.66	471.84	58.6	13.84	483.56	-65.86	13.84	494.3	-151.7	138.56	12.6957	-8.5997	72.2552
33	F	529.68	-109.9	181.66	459.34	61.1	13.84	476.06	-60.86	13.84	494.04	-160.8	126.7	27.7536	-10.552	68.377
34	F	516.64	-96.2	170.06	461.84	68.6	13.84	461.06	-43.36	13.84	477.96	-144.6	112.08	21.3134	-13.534	64.535
35	F	538.46	-125.2	175.6	476.84	43.6	12.94	483.56	-68.36	12.94	494.54	-192.2	130.7	24.1737	-14.429	66.8484
36	F	517.48	-95.06	188.88	469.34	66.1	13.84	483.56	-63.36	13.84	496.16	-158.4	101.78	17.7299	-3.2407	70.6927
37	F	530.98	-92.02	198.06	474.34	66.1	13.84	483.56	-58.36	13.84	509.64	-160.4	116.52	21.1038	-3.0329	73.5325
38	F	542.82	-110.5	173.84	491.84	68.6	12.94	488.56	-63.36	12.94	512.36	-154.8	126.1	19.4158	-10.795	66.0442
39	F	517.48	-112.5	169.06	466.84	63.6	13.84	471.06	-53.36	13.84	489.12	-153.5	118.58	19.5973	-16.442	64.6065
40	F	534.86	-100.1	185.64	471.84	73.6	13.84	478.56	-53.36	13.84	498.66	-170.5	127.06	24.3452	-9.3376	69.6328
41	F	521.38	-111.6	174.7	471.84	58.6	12.94	476.06	-58.36	12.94	483.32	-153.8	130.94	18.8623	-13.364	66.745
42	F	536.6	-110.4	171.18	469.34	63.6	13.84	471.06	-58.36	13.84	509	-169.4	127.1	26.7117	-12.672	64.5175
43	F	535.62	-120.7	191.64	486.84	46.1	13.84	488.56	-65.86	13.84	507.36	-184.7	116.08	18.0892	-12.418	72.2164
44	F	536.9	-123.5	162.54	461.84	46.1	12.94	456.06	-65.86	12.94	505.62	-168.1	107.42	30.3267	-15.221	61.3177
45	F	532	-120.7	169.74	474.34	48.6	12.94	476.06	-68.36	12.94	506.4	-175.6	105.04	22.5668	-13.216	64.695
46	F	531.32	-105.3	188.58	459.34	63.6	12.94	463.56	-50.86	12.94	488.68	-183.2	108.22	28.0868	-11.818	70.8443
47	F	533.52	-106	168.7	461.84	68.6	13.84	483.56	-58.36	13.84	495.46	-172.2	103.94	28.9432	-11.216	63.9746
48	F	537.66	-134.2	207.14	471.84	56.1	13.84	466.06	-80.86	13.84	511.26	-191.5	152.06	24.8328	-9.8242	76.7723
49	F	532.34	-118	185.2	474.34	53.6	12.94	478.56	-75.86	12.94	507.18	-188.8	117.22	22.1073	-7.5383	69.719

50	F	526.54	-112.2	192.94	466.84	56.1	12.94	466.06	-78.36	12.94	496.24	-189.5	118.3	22.4476	-3.3037	71.815
51	F	517.74	-107.2	188.16	484.34	63.6	17.24	488.56	-43.36	17.24	494.06	-156.7	111.28	12.1737	-22.45	74.2264
52	M	491.88	-90.88	201.86	484.34	73.6	17.24	486.06	-23.36	17.24	483.68	-142.3	123.52	0.01846	-22.952	79.2052
53	M	534.78	-134.5	185.38	466.84	38.6	12.94	458.56	-75.86	12.94	496.6	-187.1	105.02	27.8136	-19.098	73.3719
54	M	522.58	-87.02	190.88	469.34	81.1	15.24	468.56	-23.36	15.24	500.94	-142	103.88	21.1827	-21.524	75.3204
55	M	513.64	-110.8	190.42	479.34	58.6	17.24	486.06	-33.36	17.24	487.86	-159.8	107.04	12.5508	-28.044	75.0143
56	M	533.56	-144.9	203.92	474.34	41.1	12.94	478.56	-58.36	12.94	516.26	-216.3	575.24	23.4874	-29.75	80.8255
57	M	538.28	-113.6	187.48	461.84	56.1	12.94	463.56	-30.86	12.94	500.52	-180.6	115.24	31.6778	-29.051	74.2273
58	M	524.02	-115.9	213.8	464.34	68.6	17.24	473.56	-38.36	17.24	479.32	-171.2	117.3	23.5547	-25.627	82.8611
59	M	542.9	-87.2	188.86	474.34	71.1	12.94	466.06	-40.86	12.94	476.36	-167.5	105.24	27.9117	-13.477	74.4738
60	M	520.06	-120.2	201.16	476.84	53.6	12.94	478.56	-50.86	12.94	502.86	-157	142.62	16.3298	-23.122	80.1037
61	M	535.48	-124.5	177.74	459.34	41.1	17.24	468.56	-70.86	17.24	481.5	-178.8	104.88	32.2607	-17.884	69.3248
62	M	534.06	-117.7	196.24	471.84	66.1	12.94	468.56	-40.86	12.94	510.3	-167.9	137.18	24.9867	-26.198	77.7639
63	M	535.74	-126.7	210.18	464.34	53.6	17.24	473.56	-55.86	17.24	494.34	-188.9	122.46	28.8425	-22.815	81.2194
64	M	534.88	-140.1	191.44	469.34	38.6	13.84	468.56	-83.36	13.84	497.12	-206	125.72	26.6455	-18.07	75.5661
65	M	528.72	-108.7	193.38	466.84	53.6	12.94	473.56	-50.86	12.94	495.68	-174.5	121.74	24.9838	-18.503	76.9271
66	M	522.76	-138.2	188.5	469.34	31.1	12.94	471.06	-73.36	12.94	482.3	-202	101.9	21.2862	-22.056	75.3547
67	M	540.56	-133.4	192.72	481.84	66.1	17.24	481.06	-65.86	17.24	492.48	-199	112.38	23.6749	-23.07	75.1015
68	M	523.34	-117.7	198.44	436.84	48.6	13.84	453.56	-10.86	13.84	488.7	-175.4	119.88	35.9066	-37.95	77.9945
69	M	523.96	-108.7	205.72	459.34	58.6	17.24	461.06	-33.36	17.24	483.42	-162.9	118.7	25.9344	-25.163	79.6739
70	M	525.34	-86.7	184.62	469.34	53.6	12.94	471.06	-48.36	12.94	482.68	-166.4	107.38	22.53	-10.7	73.7124
71	M	528.74	-96.8	191.08	464.34	78.6	17.24	468.56	-38.36	17.24	487.02	-166.5	105.66	26.3322	-19.198	74.4336
72	M	532.96	-106.5	210.28	471.84	73.6	20.74	473.56	-30.86	20.74	512.18	-164.1	120.24	24.3461	-25.274	80.1578
73	M	527.74	-93.74	208.94	479.34	71.1	18.34	478.56	-35.86	18.34	491.32	-162	136.5	18.5803	-17.921	80.6812
74	M	538.86	-107.9	178.84	449.34	56.1	17.24	456.06	-28.36	17.24	495.48	-170.5	105.2	38.1005	-28.364	69.0286
75	M	534.26	-120.9	204.72	484.34	53.6	12.94	486.06	-60.86	12.94	481.18	-192.5	117.5	19.2502	-18.745	81.1304
76	M	541.02	-110.8	206.74	476.84	61.1	15.54	488.56	-38.36	15.54	499.56	-173.7	120.88	25.7235	-23.837	80.8738

77	M	530.18	-123.6	201.2	469.34	46.1	17.24	468.56	-63.36	17.24	497.6	-181.5	128.04	24.3412	-19.207	78.016
78	M	522.46	-129.9	204.12	481.84	38.6	13.84	486.06	-65.86	13.84	496.32	-186.2	134.7	15.1108	-20.757	80.883
79	M	528.12	-117.1	201.68	484.34	66.1	17.24	486.06	-40.86	17.24	487.88	-177	116.52	16.6717	-26.334	78.7815
80	M	510.64	-98.1	187.24	481.84	61.1	17.24	491.06	-38.36	17.24	499.04	-150.4	141.06	10.0427	-20.819	74.0233
81	M	524	-133.1	200.48	461.84	56.1	17.24	468.56	-35.86	17.24	488.8	-195.3	106.4	25.0462	-34.772	78.0069
82	M	518.96	-130	215.2	451.84	38.6	12.94	473.56	-63.36	12.94	492.16	-186.6	121.26	26.7249	-20.525	84.8367
83	M	515.28	-91.84	197.16	481.84	76.1	12.94	476.06	-35.86	12.94	498.8	-146.8	153.14	11.9206	-17.816	78.6831
84	M	520.74	-93.14	182.76	466.84	66.1	13.84	473.56	-40.86	13.84	484.56	-148.2	125.02	21.7465	-17.207	73.0758
85	M	507.82	-107.3	200.52	481.84	56.1	15.54	491.06	-63.36	15.54	485.66	-164.7	129.02	8.50062	-12.627	79.1091
86	M	531.18	-94.48	196.22	466.84	51.1	13.84	481.06	-48.36	13.84	502.5	-158.8	136.14	26.0486	-13.276	77.6234
87	M	532.94	-92.5	203.52	489.34	81.1	17.24	486.06	-38.36	17.24	506.86	-165.8	139.04	16.5007	-16.717	79.2032
88	M	513.02	-118.1	199.54	459.34	51.1	13.84	466.06	-53.36	13.84	489.06	-170.7	128.4	21.1383	-21.219	79.0511
89	M	526.22	-99.58	191.34	486.84	58.6	13.84	486.06	-48.36	13.84	499.98	-152.5	146.32	14.783	-16.243	76.2797
90	M	521.78	-106.3	192.42	476.84	68.6	13.84	471.06	-43.36	13.84	485.86	-164.1	138.14	17.2922	-21.099	76.4756
91	M	525.62	-92.32	196.28	474.34	78.6	13.84	473.56	-28.36	13.84	490.08	-156.5	126.42	20.0998	-21.128	77.7913
92	M	500.9	-123.1	190.88	464.34	48.6	13.84	468.56	-60.86	13.84	489.82	-151.3	129.5	13.5206	-21.161	76.3221
93	M	533.76	-127.3	190.06	461.84	58.6	12.94	476.06	-55.86	12.94	501.22	-167	132.06	29.7053	-24.409	75.6789
94	M	527.02	-115.1	193.5	444.34	31.1	13.84	448.56	-58.36	13.84	498.58	-180.6	115.9	34.1979	-17.45	75.8103
95	M	538.26	-106.1	216.52	484.34	53.6	13.84	481.06	-65.86	13.84	508.2	-177.8	129.62	20.649	-9.313	84.3755
96	M	513.5	-108	191.98	466.84	61.1	13.84	466.06	-40.86	13.84	496.44	-146.8	130.52	18.1183	-22.967	76.406
97	M	528.18	-104.3	195.68	479.34	76.1	13.84	478.56	-43.36	13.84	500.7	-157.4	133.88	19.007	-19.917	77.628
98	M	544.36	-121.2	186.88	474.34	71.1	13.84	476.06	-43.36	13.84	511.36	-188.2	109.94	28.8739	-27.354	73.9119
99	M	541.4	-106.3	191.36	464.34	78.6	13.84	466.06	-38.36	13.84	509.04	-158.5	121.38	31.8179	-22.552	75.2541
100	M	539.66	-122	192.12	474.34	63.6	13.84	478.56	-48.36	13.84	503.34	-168.3	136.92	26.6034	-25.323	76.0464
101	M	557.24	-128.5	183.16	464.34	58.6	13.84	471.06	-50.86	13.84	507.28	-189.4	107.72	39.2144	-26.821	71.7799
102	M	536.1	-113.5	208.2	481.84	53.6	13.84	478.56	-60.86	13.84	505.52	-180.2	150.86	21.0676	-15.232	81.7111

Appendix C

Ischial Tuberosity Location

In this appendix the technique for locating the ischial tuberosity using a pressure mat system was verified by comparing the results to those from radiographic measurements of the pelvis for a single subject. In addition, the tissue between the ischial tuberosity and the seat surface was measured from the same radiograph.

Methods: A Tekscan pressure mat system was used to record the pressure of a subject while seated on a hard surface. Almost simultaneously, a lateral pelvic radiograph was taken of the subject. The pressure mat system was positioned so that it was in line with the central ray of the X-ray. The entire pelvis and pressure mat below the pelvis were visible on the radiograph. Due to the metallic content of the pressure mat design, the individual cells of the pressure mat were also visible. In addition, two metal spheres 1mm in diameter were fixed to a radiolucent frame and placed just lateral to the pelvis to provide a means of calibrating the distances measured on the radiograph. The true distance between the two spheres was measured using calipers and the distance between the spheres on the radiograph was divided by the true distance, providing a correction factor for radiographic measurements.

Results: The lowest point of the ischial tuberosity was measured relative to the posterior of the pressure mat using a set of calipers. The measurement was repeated 7 times, with an average of 63.0mm (range 61.9mm - 64.5mm). The peak pressure from the pressure data was calculated using the methods described in this report and was 65.0mm from the posterior of the pressure mat.

The tissue thickness was calculated by measuring from the most inferior point on the ischial tuberosity to the surface of the pressure mat visible on the radiograph. This measurement was repeated 4 times, with an average of 11.8mm (range 11.4mm - 12.2mm).

Discussion: The difference between the pressure mat method for locating the ischial tuberosity and a radiographic method is approximately 2mm. The distance between the cells of the pressure mat are 2.5mm; thus, it can be concluded that the pressure mat system for locating the ischial tuberosity is accurate to the cell size of the pressure system.

Tissue thickness measurements are between 11.4mm - 12.2mm for a subject 179.5cm tall and 82Kg. The subject is average weight for his stature and he has average to below-average tissue in the buttock region. It can be concluded that the tissue between the ischial tuberosity and the seat is between 10-15mm for subjects having an average weight for their height. For subjects heavier than the average weight for their height, it is likely that the tissue thickness is greater.